INTERACTIONAL APPROACH OF CANTILEVER PILE WALLS ANALYSIS

STANISLAV ŠKRABL

About the author

Stanislav Škrabl
University of Maribor,
Faculty of Civil Engineering
Smetanova ulica 17, 2000 Maribor, Slovenia
E-mail: stanislav.skrabl@uni-mb.si

Abstract

This paper proposes a new method for the geomechanical analysis and design of cantilever retaining structures. It is based on the limit equilibrium method, but it uses some additional conditions for interaction between the retaining structure and the ground, when referring to the distribution of the mobilized earth pressures on the structure. The greatest benefit of the proposed method is shown in the analysis of structures of layered ground (heterogeneous above the dredge level and homogeneous below it), embedded in frictional and cohesive materials, and in the possibility of considering the influence of surcharge loadings on the active or passive side of the retaining structure. When analyzing such cases in practice, the proposed method gives results which are in better agreement with the results of FEM based elasto-plastic interaction analyses than with the results of currently used methods. At the same time, its results are in accordance with those published for homogeneous cohesionless ground. Since in practice almost all retaining structures are erected in layered ground (heterogeneous above the dredge level and homogeneous below it), the proposed method is very convenient and applicable for the analyses and design of cantilever structures under arbitrary geomechanical conditions.

Keywords

retaining walls, embedment, cantilevers, soil-structure interaction, earth pressure, pressure distribution, wall friction, limit analysis, shear forces

1 INTRODUCTION

In geotechnical practice, cantilever embedded retaining structures are specifically used for protecting permanent and temporary excavations, for highway construction, and sanitation of landslides. These structures are mostly sheet walls as temporary retaining structures, and pile walls and diaphragms as permanent retaining structures.

Embedded retaining structures sustain overturning moments and horizontal forces, which are caused by backfill soil, ground water and surcharge loading. The contact pressures and resistances are distributed over the embedment depth due to the backfill loading, so that the entire retaining structure remains in equilibrium. The limit state of the retaining structure is achieved when the distribution of contact pressures and extensive regions of plastification in the ground are re-established at the embedded part of the structure, and the structure is no longer capable of taking additional backfill loading. The limit state can be defined by the limit shear loading of the ground or bending moment and shear loading of the retaining structure, respectively. Therefore, only retaining structures, which have a comparable level of safety and reliability for the ultimate limit state of both the soil and the structure, can be optimal.

Bica and Clayton (1989) describe several different methods for the geomechanical analysis and design of embedded retaining structures. In these methods, different assumptions of soil pressure distribution, deformations and wall displacements are considered over the embedded part of the retaining structure. Most of the considered methods are limit equilibrium methods. They are based on a classical distribution of the limit soil pressure values. Some model studies of retaining structures are well known, e.g. Rowe (1951), Lyndon and Pearson (1985), Bica and Clayton (1993), as well as some empirical methods for the design of retaining structures.

King (1995) proposed an original approach to geomechanical analysis in homogenous cohesionless soil, which is based on the method of limit equilibrium,

polygonal distribution of soil pressures and one empirically determined parameter. This parameter is the depth, at which the net pressure is vanishing. King defined this depth by centrifuge test results. Day (1999) suggested improving King's method by determining the empirical parameter using the results of FEM analysis. Both methods, King's and Day's, are applicable only to analyses of retaining structures in homogeneous cohesionless ground without additional surcharge loading. This paper firstly presents a generalization of the existing standard methods for the analyses of rigid retaining structures embedded in frictional and cohesive layered ground (heterogeneous above the dredge level and homogeneous below it) with surcharge loading, and then compares the obtained results with the results of FEM-based analyses. Finally, it proposes a new method that considers significant interactive conditions between the retaining structure and the ground.

2 GENERALIZATION OF CURRENT USED METHODS

The aim of the analyses based on the method of limit equilibrium is to determine the critical excavation depth and the critical values of bending moment and shear force at which the limit equilibrium state can be reached. The first important step of this approach is to determine the soil pressure, which can be activated at the ultimate limit state of the ground.

The soil pressures acting on the retaining structure at the ultimate limit state, depends on the complex properties of the interaction between the retaining structure and the ground. The most important interaction parameter represents equal displacements of both mediums along the contact surface between the retaining structure and the ground. As a rule, the retaining structures are designed by the limit values of soil pressures which cannot be activated over the whole region of interaction due to the condition of both mediums' equal displacements. The general shape of the mobilized earth pressures acting at the ultimate limit state of the homogeneous cohesionless ground is presented in Fig. 1. All standard methods are based on earth pressures at limit equilibrium. Methods differ only in the assumptions and simplifications used in the determination of these pressures.

A generalization of the existing methods to the case of a layered strata is presented in this section. Layered strata means multilayer above the dredge level and a single layer below it.
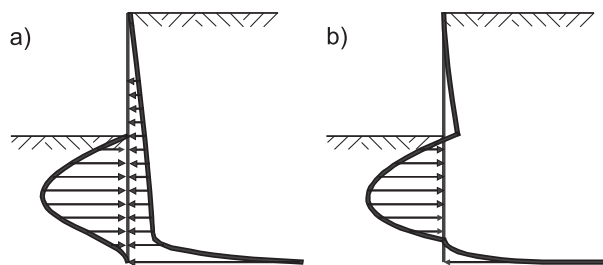

Figure 1. Activated Influences and Resistances: (a) Soil Pressure Distribution; (b) Net Soil Pressure Distribution

2.1 UK SIMPLIFIED METHOD[GE]

This method, mostly used in Europe, is the simplest one. It is described in several publications (Padfield and Mair 1984, King 1995), and represents the basis of many computer codes for designing embedded retaining structures. The activation of all active pressures and passive resistances in this method is assumed, above the calculating rotation point 1 (Fig. 2). The resistances under the rotation point are not determined exactly; they are substituted with the fictitious concentrated force R.
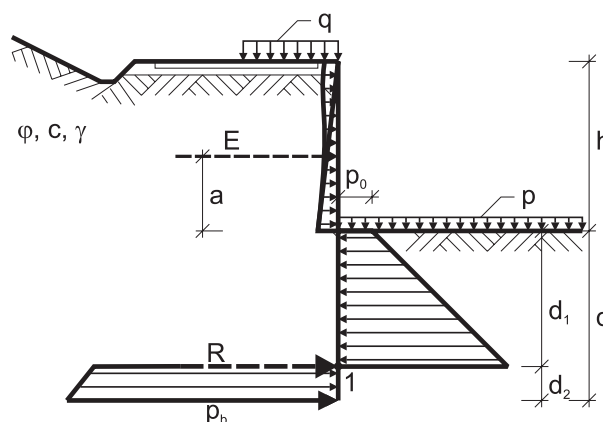

Figure 2. Influences and Resistances According to the UK Simplified, and UK Full Method

By considering the equilibrium condition of the moments around the rotation point 1, we obtain:

$$d_1^{*3}(K-1)+1.5p_0^*d_1^{*2}-3E^*(a^*+d_1^*)=0 \quad (1)$$

where the normalized quantities are:

$$d_1^* = d_1/h, \quad K = K_{p\gamma}/K_{a\gamma},$$
$$E^* = 2E/(\gamma h^2 K_{a\gamma}), \quad c^* = 2c/(\gamma h)$$
$$p_0^* = c^*\left(K_{ac}+K_{pc}\right)\!/K_{a\gamma} + p^* K_{pq}/K_{a\gamma} - 2, \quad (2)$$
$$q^* = 2q/(\gamma h), \quad a^* = a/h$$

$K_{a\gamma}$, K_{py}, and K_{ac}, K_{pc}, and K_{pq} denote the coefficients of active and passive pressures for the influences of soil weight, cohesion and surcharge (Kérisel and Absi 1990). The letters γ, c and q in indices denote the unit weight, cohesion and surcharge loading of the soil layer in which the analyzed retaining structure is embedded. The required embedment depth d_1 up to point 1 is determined by solving (1). The analytical solution (3) can be applied only for a retaining structure in homogeneous cohesionless soil without surface or other additional loading.

$$d_1^* = 1/(\sqrt[3]{K} - 1) \qquad (3)$$

The total required embedment depth $d = d_1 + d_2$ is approximately:

$$d^* = 1.2 d_1^*, \quad d^* = d/h \qquad (4)$$

The maximum values of bending moment and shear force acting on the retaining structure are determined:

$$M_m = M_m^* \gamma h^3 K_{a\gamma}/2, \qquad T_m = T_m^* \gamma h^2 K_{a\gamma}/2 \qquad (5)$$

where M_m^* and T_m^*, are the normalized values of the maximum inner forces determined by using:

$$M_m^* = E^*(a^* + x_m^*) - p_0^* x_m^{*2}/2 - (K-1)x_m^{*3}/3$$
$$T_m^* = E^* - p_0^* d_1^* - (K-1)d_1^{*2} \qquad (6)$$

where x_m^* denotes the distance between the point where the maximum bending moment acts and the dredge line:

$$x_m^* = \frac{(p_0^{*2} + 4(K-1)E^*)^{1/2} - p_0^*}{2(K-1)} \qquad (7)$$

2.2 UK FULL METHOD[GE]

UK full method additionally considers the influence of limit pressures under rotation point 1 (Fig. 2). The ground resistance at the toe of the embedded wall is determined:

$$p_b^* = 2p_b/(\gamma h K_{a\gamma}) = 2K\gamma^* + 2(K-1)d^* + c^*(K_{pc} - K_{ac})/K_{a\gamma} \qquad (8)$$

where γ^* denotes the ratio of the average unit weight of the backfill ground above the dredge line for the considered problem to the unit weight of the ground under the dredge line.

After considering the equilibrium conditions of the horizontal forces and moments we obtain the following expressions:

$$d_2^* = ((K(\gamma^* + d_1^*) - d_1^* + c^*(K_{pc} + K_{ac})/2K_{a\gamma})^2/(K-1)^2 +$$
$$((K-1)d_1^{*2} + p_0^* d_1^* - E^*)/(K-1))^{1/2} \qquad (9)$$
$$-(K(\gamma^* + d_1^*) - d_1^* + c^*(K_{pc} + K_{ac})/2K_{a\gamma})/(K-1)$$

$$E^*(3a^* + 3d_1^* + 2d_2^*) - p_0^* d_1^*(1.5d_1^* + 2d_2^*) + K\gamma^* d_2^{*2}$$
$$-(K-1)(d_1^{*3} + 2d_1^{*2} - d_1^* d_2^{*2}) + 0.5c^*(K_{pc} + K_{ac})d_2^{*2}/K_{a\varphi} = 0 \quad (10)$$
$$d_2^* = d_2/h$$

The required embedment depth $d = d_1 + d_2$ is calculated by solving the system of equations (9) and (10). The maximum values of bending moment and shear force acting on the retaining structure are determined using (5), (6) and (7).

2.3 USA METHOD[GE]

The USA method, which was first introduced by Bowles (1988) for homogeneous soil, supposes that the entire passive resistance is mobilized at the toe of the retaining structure. In the region between depths d_1 and d (Fig. 3), the resulting resistances have the form of a straight line (polygonal net pressure distribution).
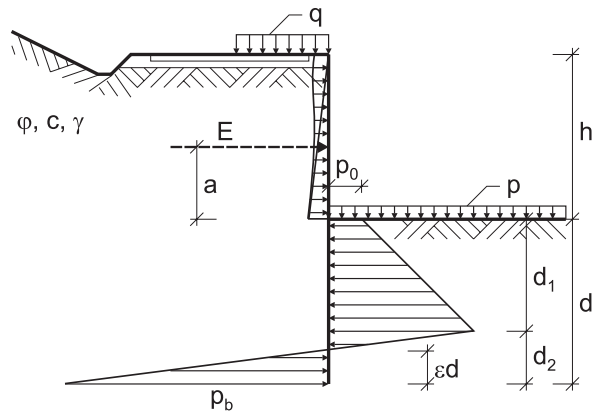

Figure 3. Influences and Resistances According to the USA, King, and Day Methods

The individual earth pressures and available passive pressures above the calculated embedment depth can be estimated for arbitrarily layered ground. The unknown embedment depth d in the soil at the toe of the pile wall is determined by using the equilibrium of horizontal forces (11), while the depth d_1 is determined by the moment equilibrium condition (12).

$$E^* + (\gamma^* K + (K-1)d^* + 0.5c^*((K_{pc} + K_{ac})/K_{a\gamma})(d^* - d_1^*) -$$
$$0.5p_0^*(d^* + d_1^*) - (K-1)d^* d_1^* = 0 \qquad (11)$$

$$d_1^* = (E^*(3a^* + 2d^*) - 0.5p_0^* d^{*2})/((K-1)d^{*2} - E^* + p_0^* d^*) \quad (12)$$

2.4 KING'S METHOD[GE]

On the basis of centrifuge model tests, King (1995) established that not all available resistances at the toe of an embedded pile without anchors could be fully activated in the limit state. He, therefore, proposed modifying the USA method by considering a polygonal form of the active and passive pressures, and determining experimentally the value of parameter $\varepsilon = 0.35$. This parameter defines the depth at which the activated contact-stresses in front of and behind the embedded pile are balanced. King only gave solutions for homogeneous cohesionless ground. The critical embedment depth d for layered ground can be determined using (13).

$$E^*(d^*(1-\varepsilon)-d_1^*)-0.5p_0^*(d^{*2}(1-2\varepsilon)-d_1^{*2})-$$
$$(K-1)d^*d_1^*(d^*(1-2\varepsilon)-d_1^*(1-\varepsilon))=0 \qquad (13)$$

The depth d_1 is determined by the moment equilibrium condition (12).

2.5 DAY'S METHOD[GE]

Day (1999) found that King's method gave too conservative results, particularly for lower values of parameter K. If K is lower than 7.90, the solution does not practically exist.

He therefore proposed, on the basis of the interaction analysis results using FEM, introducing new value of parameter ε.

$$\varepsilon = 0.047\ln(K)+0.1 \qquad (14)$$

In Day's method the unknown embedment depth is also determined using (12) and (13).

3 FINITE ELEMENT ANALYSESS

A set of two-dimensional plane strain analyses for the ultimate limit state of embedded retaining structures was performed to confirm the results of the described analytical methods. The critical excavation depth was determined by progressive removal of the excavated soils until the horizontal displacement of the wall was so high that further re-establishment of the retaining structure's global equilibrium could not occur anymore.

A relatively stiff elastic concrete retaining structure of the total length $h + d = 10.0$ m was considered in the analyses. Its characteristics were $E = 31\cdot10^6$ kPa, $I = 0.083$ m^4/m and $A = 1$ m^2/m. The cross-section of the analyzed excavation is presented in Fig. 4.
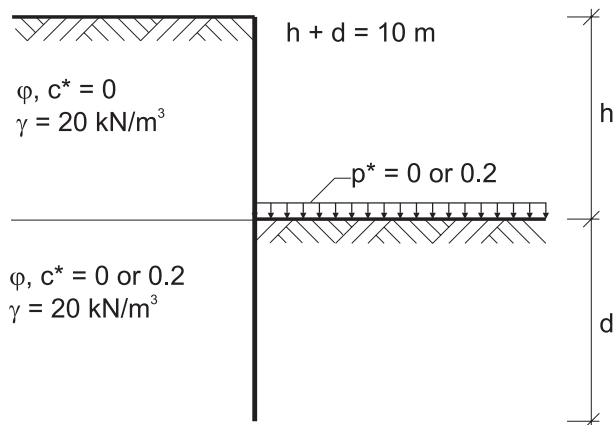

Figure 4. Cross-Section of the Analyzed Excavation

The elasto-plastic Hardening-Soil model with isotropic hardening (PLAXIS 1998) was used. The advantage of the Hardening-Soil model over the Mohr-Coulomb model is in the use of a hyperbolic stress-strain curve, and the stress dependency on soil stiffness. The Hardening-Soil model uses the theory of plasticity, includes dilatancy and introduces a cap yield surface. The following properties were considered: $E_{50}^{ref}=E_{oed}^{ref}= 40$ MPa, $E_{ur}^{ref} = 3E_{50}^{ref}$, $v_{ur}= 0.2$, $m = 0.5$, $R_f= 0.9$, $p^{ref}= \gamma h$, where h denotes the final excavation depth in the limit state. The analyzed region was discretized in 2.000 six-node triangle finite elements with a refined mesh near the retaining structure. The finite element mesh with the deformed mesh of the analyzed excavation is presented in Fig. 5.
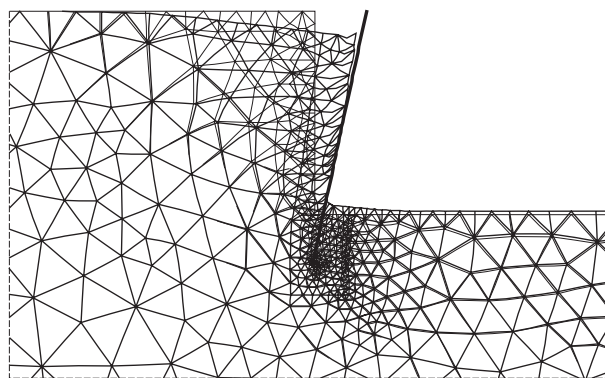

Figure 5. The Cutting Out of the Finite Element Mesh with the Deformed Mesh (scaled 10 times) of the Analyzed Excavation

The numerical analyses were performed for friction angles $\varphi =10°$ to $\varphi =50°$ in steps of 5°, normalized cohesions $c^*=0$ and 0.2, and normalized surcharges $p^*=0$ and 0.2. All analyses considered the friction between the retaining structure and the ground $\delta = \varphi$, dilatation $\psi = \varphi/2$ and unit weight of soil $\gamma = 20$ kN/m^3.

The ultimate limit state, reflected in the critical excavation depth h_c, was considered as a state when no equilibrium could be ensured anymore or when numerical results could not converge.

The results of analyses have shown that the deformations obtained for the used elasto-plastic soil model for a rigid retaining structure are directly proportional to the square of the excavation, and inversely proportional to the deformation modulus E_{50}. The displacements of the retaining structure can be determined using (15).

$$u = u^* \gamma\, h^2 / E_{50} \qquad (15)$$

where u is the displacement of the actual structure and u^* the displacement determined on a generalized system with normalized quantities $h^* = h / h = 1$, $d^* = d / h$, $t^* = t / h$, $\gamma^* = 1$, c^*, q^* and p^*, where t is the thickness of the retaining wall. The actual values of maximum bending moments and shear forces can be determined on the basis of their normalized values using (6).

Variation in the normalized values of the horizontal displacements at the top of the retaining structure u^*_o with arbitrary excavation depths h^* for $p^* = q^* = c^* = 0$ (see Fig. 4) are shown in Fig. 6a. Variation in the normalized values of displacements u^*_o with arbitrary excavation depths h^* for $p^*=q^*=0$ and $c^*=0.2$ are presented in Fig. 6b, and for $q^*=c^*=0$ and $p^*=0.2$ in Fig. 6c.

The results of numerical simulations have shown that at higher friction angles the bearing capacity limit state occurs at smaller excavation depths than those determined by classic methods (UK simplified, UK full and USA). King (1995) and Day (1999) drew similar conclusions. Only in the case where $p^*= q^*= c^*= 0$ are the results of FE analyses comparable with the results of King's and Day's solutions. The differences are considerable, especially for the required embedment depth (ultimate limit state of the ground), and for the maximum internal shear forces of the retaining structures (section strength limit state of the retaining structures). The deviations are observed for retaining structures in homogeneous and layered ground, as well as for surcharges.

In geotechnical practice, retaining structures are most frequently embedded in soils of relatively high shear strength. Therefore, the choice of method for geomechanical analysis is often decisive for safety, as well as for the economy of the designed retaining structure. For this reason, the next section presents a new method which yields more reliable results. It makes it possible to design retaining structures of comparable safety for the ultimate limit state of the ground, as well as for the section strength limit states of the retaining structures.
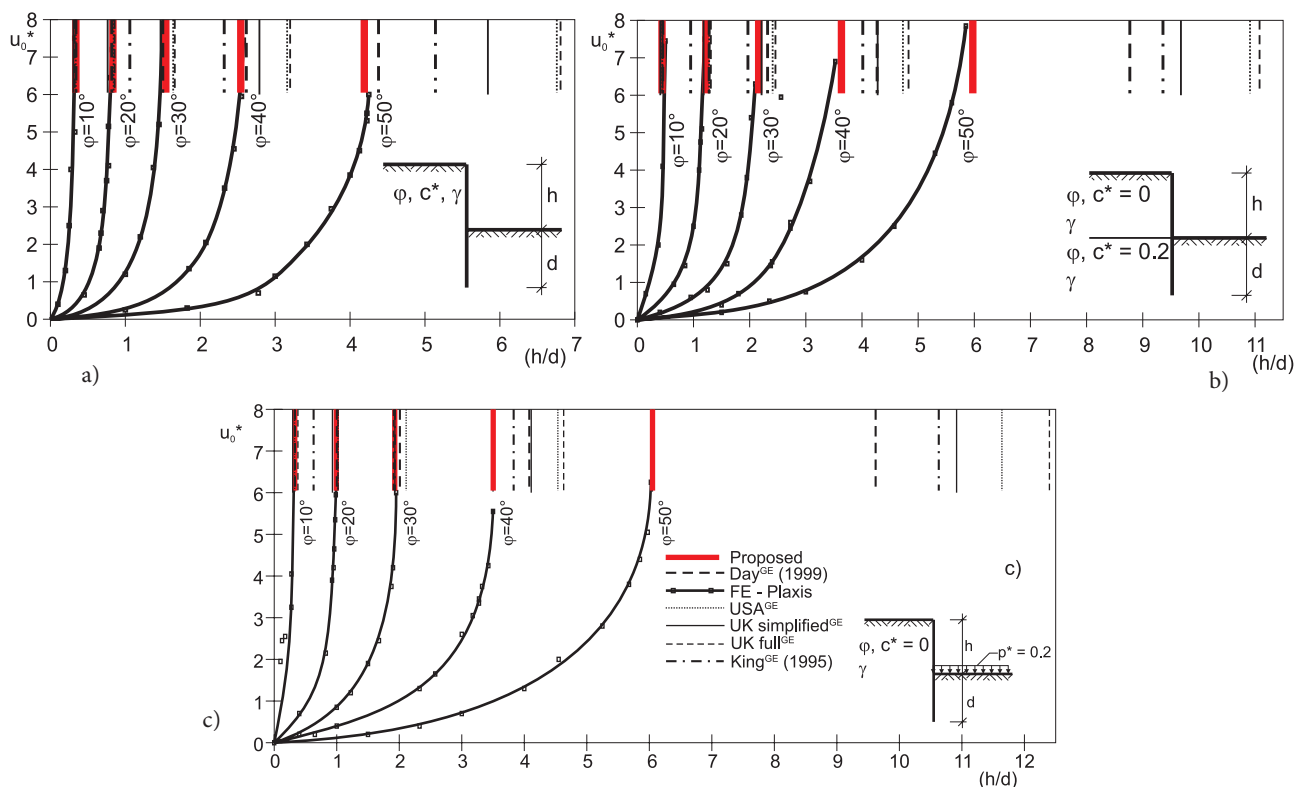

Figure 6. Normalized Values of Displacements u^*_o for: a) $p^* = q^* = c^* = 0$; b) $p^* = q^* =0$, $c^* = 0.2$; c) $q^* = c^* = 0$, $p^* = 0.2$

4 PROPOSED METHOD

Classical methods of numerical analysis (UK simplified, UK full and USA) suppose that all available passive earth pressures are mobilized in the region of embedment in the limit state of the retaining structure. The results of more recent researches (King 1995 and Day 1999) show that these resistances could not actually be mobilized as ideally as was expected. Therefore, King (1995) and Day (1999) proposed some changes in net pressure diagram. However, their approaches only ensure good results for ideal cases of retaining structures in homogeneous cohesionless ground without surcharge loading.

The proposed method is based on the results of an experimental investigation into the resistance activation in the region of the embedded part of the retaining structure at forced displacements (Fang et al. 1994). It considers the results of numerical analyses according to FEM (Day 1999), and partly the results of centrifuge tests (King 1995). The data of experimental investigation from Fang et. al 1994 were used to choose the shapes of resistances, while the data from FE analyses were used to adjust assumed parameters p_b, m and n with the results of FE analyses at the limit state.

The results of small scale laboratory experiments (Fang et al. 1994) show that resistances at the embedded part are activated in polygonal shape only at the translational displacements of the wall, and only in those cases where they approximately correspond to the passive resistance. If the wall rotates, the resistance is activated in the shape of exponential functions. The shape and the magnitude depend on the position of the rotation point and on the magnitude of the forced displacement. Fang et al. (1994) presented the experimentally determined the shapes of the activated resistances at the wall rotations around the upper and lower points.
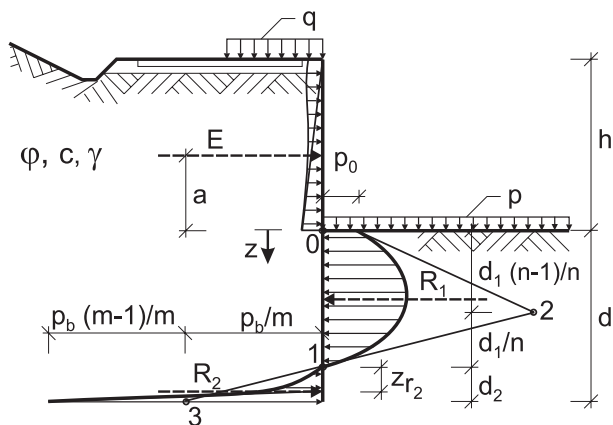

Figure 7. Influences and Activated Resistances at Limit State

The results of FE analyses show that at the limit state the rigid retaining structure rotates around the point at the depth d_1. For all analyzed cases this point is located approximately at the depth where the pressures on the wall from left and right are equal. Therefore, it can be supposed that net pressure under dredge level is mobilized in the shape of two exponential functions as presented in Fig. 7.

From the experimental research results of Fang et al. (1994), it can be assumed that the total passive resistance (p_0) is mobilized at the excavation depth, and further up to the depth (d_1) it has the form of the following function:

$$p(z) = p_0 + C_1(z/d_1) + C_2(z/d_1)^n \quad (16)$$

where C_1 and C_2 are constants determined by boundary conditions (17) and (18).

$$p(z = d_1) = p_0 + C_1 + C_2 = 0 \quad (17)$$

$$\left. \frac{dp(z)}{dz} \right|_{\substack{z=0 \\ n>1}} = \frac{C_1}{d_1} = \gamma(K_{p\gamma} - K_{a\gamma}) \quad (18)$$

After solving (17) and (18) we obtain:

$$C_1 = \gamma(K_{p\gamma} - K_{a\gamma})d_1 \quad (19)$$

$$C_2 = -p_0 - \gamma(K_{p\gamma} - K_{a\gamma})d_1 \quad (20)$$

The boundary values of (18) that can only appear at the embedment in cohesive ground or when surcharge loading is in front of the retaining structure are:

$$\left. \frac{dp(z)}{dz} \right|_{\substack{z=0 \\ n=1}} = \left(\frac{C_1}{d_1} + \frac{C_2 n z^{n-1}}{d_1^n} \right) \Bigg|_{\substack{z=0 \\ n=1}} = -\frac{p_0}{d_1} \quad (21)$$

$$\left. \frac{dp(z)}{dz} \right|_{\substack{z=0 \\ n<1}} = \left(\frac{C_1}{d_1} + \frac{C_2 n z^{n-1}}{d_1^n} \right) \Bigg|_{\substack{z=0 \\ n<1}} = -\infty \quad (22)$$

It has to be noted that the infinite slope boundary condition in (22) can only appear for higher cohesion or surcharge loading with a simultaneously high friction angle. The distribution of the mobilized earth pressures in the whole region of the embedment depth d_1 follows the exponential function given below:

$$p^*(z) = \frac{2p(z)}{\gamma h K_{a\gamma}} = p_0^* + 2(K-1)d_1^*(\frac{z}{d_1}) - (p_0^* + 2(K-1)d_1)(\frac{z}{d_1})^n \quad (23)$$

The resulting horizontal force and moment around point 0 of the mobilized earth pressures are given in (24) and (25).

$$R_1^* = p_0^* d_1^* (\frac{n}{n+1}) + (K-1)d_1^{*2}(\frac{n-1}{n+1}) \quad (24)$$

$$M_{R_1^*}^{*0} = p_0^* d_1^{*2} (\frac{n}{2(n+2)}) + 2(K-1)d_1^{*3}(\frac{n-1}{3(n+2)}) \quad (25)$$

In the region of embedment depth d_2 the following distribution of earth pressures is considered:

$$p(z) = p_b (\frac{z-d_1}{d_2})^m \quad (26)$$

where p_b denotes the horizontal pressure on the wall at the toe of the retaining structure. The resulting horizontal force of the pressures in the region of depth d_2 is given in (27), and the distance of the resulting horizontal force from point 1 in (28).

$$R_2^* = p_b^* (\frac{d_2^*}{m+1}) \quad (27)$$

$$z_{R_2}^* = d_2^* (\frac{m+1}{m+2}) \quad (28)$$

Different values of parameters p_0^*, p_b^*, $(K-1)$, m and n define a family of exponential functions that agrees with the experimental distribution of pressures along the embedment depths of the rigid retaining structures.

The values of parameters m and p_b^* are determined from the results of numerical simulations of the limit states of retaining structures embedded in cohesionless and layered ground, as well as for the case of surcharge loading in front of the retaining structure. Parameter m is based on numerical interpolation using results of elasto plastic analyses using FEM and can be expressed as:

$$m = 2 + \ln(K)/4 \quad (29)$$

The comparative value of parameter p_b^* is determined experimentally for individual numerical solutions at the ultimate limit state:

$$p_b^* = \frac{|T_m^*|(m+1)}{d_2^*} \quad (30)$$

where T_m^* denotes the maximum normalized shear force acting on the retaining structure at limit state determined using FEM. The numerically (using FEM) and analytically (using Eq. 31) determined values of parameter p_b^* are presented in Fig. 8.
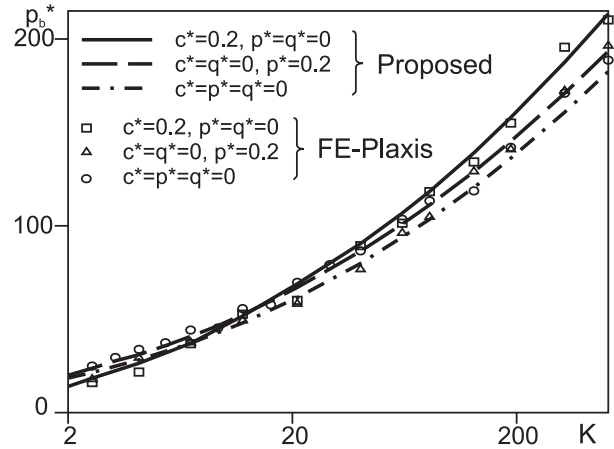

Figure 8. Numerical and Analytical Values of Parameter p_b^*

In the analysis of retaining structures we can consider the following normalized values of pressures at the toe of the pile wall in a wider region of the value K (Fig. 8):

$$p_b^* = (1 + d^* + c^*)(\ln K + 3.8\ln^2 K) \quad (31)$$

Equation (31) is the approximation of the results using FEM determined by method of the least square. The mobilized pressures in front of and behind the retaining structure (defined by parameters n and m) are linked with (32). The relationship is determined by the slope of the tangent (line 2-3, see Fig. 7) to the net pressure function in front of the retaining structure through point 1.

$$n = \frac{p_b^* d_1^* / m + 2(K-1)d_1^* d_2^*}{p_0^* d_2^* + 2(K-1)d_1^* d_2^*} \quad (32)$$

The embedment depths of the retaining structure d_1^* and d_2^* are determined considering the moment equilibrium around point 1 (33), and the horizontal forces' equilibrium condition (34).

$$E^*(a^* + d_1^*) - p_0^* d_1^{*2}(\frac{n}{n+1} - \frac{n}{2(n+2)})$$
$$-(K-1)d_1^{*3}(\frac{n-1}{n+1} - \frac{2(n-1)}{3(n+2)}) - p_b^* \frac{d_2^{*2}}{m+2} = 0 \quad (33)$$

$$E^* - p_0^* d_1^* (\frac{n}{n+1}) - (K-1)d_1^{*2}(\frac{n-1}{n+1}) + p_b^* d_2^* /(m+1) = 0 \quad (34)$$

The required embedment depth d^* and the parameter n, representing the stage of pressure mobilization along the embedment depth d_1^*, are determined for each considered case separately by solving a system of three nonlinear equations (32), (33) and (34). The maximum bending moment and shear force acting on the embed-

ded retaining structure at limit state are determined using (35) and (36).

$$T_m^* = E^* - p_0^* d_1^* (\frac{n}{n+1}) - (K-1)d_1^{*2}(\frac{n-1}{n+1}) \quad (35)$$

$$M_m^* = E^* (a^* + x_m^*) - p_0^* x_m^{*2}(\frac{1}{2} - \frac{x_m^n}{d_1^{*n}(n^2+3n+2)}) - \quad (36)$$
$$(K-1)x_m^{*3}(\frac{1}{3} - \frac{2x_m^{n-1}}{d_1^{n-1}(n^2+3n+2)})$$

The distance of point x_m, where the maximum bending moment acts, from the toe of the excavation is determined using (37).

$$E^* - p_0^* x_m^*(1 - \frac{x_m^n}{d_1^{*n}(n+1)}) - (K-1)x_m^{*2}(1 - \frac{2x_m^{n-1}}{d_1^{n-1}(n+1)}) = 0 \quad (37)$$

Numerical procedure

i)   We determine $K = K_{py} / K_{ay}$; $E^* = 2E/(\gamma h^2 K_{ay})$; $a^* = a/h$, $p_0^* = 2p_0/(\gamma h K_{ay})$, $m = 2 + \ln(K)/4$

ii) Using Microsoft Solver real minimum solution of $d_1^* + d_2^*$ of nonlinear equations (31) - (34) with constraints ($d_1^* > 0$ and $+ d_2^* > 0$).

iii) For obtained values d_1^* and d_2^* the position of maximum bending moment x_m^* (Eq 37) and values of maximum shear force T_m^* (Eq 35) and maximum bending moment M_m^* (Eq 36) are determined. For case $c^* = q^* = p^* = 0$ of geomechanical analysis for shear angles $\varphi = 15°$, $20°$, $25°$, $30°$, $35°$, $40°$, $45°$, and $50°$ are given in Table 1.

Table 1. The Results of Analyses for $\delta /\varphi = 1$, for $c^* = q^* = p^* = 0$

φ [°]	p_b^*	m	n	d_1^*	d_2^*	M_m^*	T_m^*
(1)	(2)	(3)	(4)	(5)	(6)	(7)	(8)
15	26.012	2.355	8.713	1.5630	0.2957	1.2892	2.293
20	36.708	2.488	8.252	1.0273	0.2060	0.8586	2.168
25	48.997	2.621	7.243	0.7302	0.1592	0.6594	2.155
30	63.926	2.762	5.996	0.5359	0.1297	0.5452	2.203
35	83.642	2.925	4.656	0.3942	0.1082	0.4703	2.306
40	108.645	3.102	3.472	0.2953	0.0927	0.4226	2.454
45	142.887	3.311	2.489	0.2224	0.0802	0.3905	2.657
50	191.143	3.559	1.774	0.1705	0.0697	0.3697	2.924

Table 2. The Results of Analyses for Different Combinations of h and p values

			Method						
			UK Simpl.	UK Full	USA	King	Day	FE	Proposal
(1)	(2)	(3)	(4)	(5)	(6)	(7)	(8)	(9)	(10)
(a) h=10.0 m, p=0									
Total wall height	$h+d$	(m)	11.77	11.52	11.53	12.01	12.32	12.44	12.43
Max. shear force	T_m	(kN/m)	910.2	854.0	766.5	389.9	310.0	302.1	297.3
Max. bending moment	M_m	(kNm/m)	373.3	373.3	373.8	373.3	373.3	379.3	377.9
(b) h=10.5 m, p=10 kPa									
Total wall height	$h+d$	(m)	11.85	11.67	11.68	11.92	12.03	12.56	12.52
Max. shear force	T_m	(kN/m)	1011.7	945.5	860.5	559.2	491.3	366.0	317.3
Max. bending moment	M_m	(kNm/m)	404.7	404.7	404.7	404.7	404.7	410.6	406.2
(c) h=11.0 m, p=20 kPa									
Total wall height	$h+d$	(m)	12.14	12.01	12.02	12.17	12.24	12.92	12.89
Max. shear force	T_m	(kN/m)	1205.4	1115.7	958.1	735.9	664.3	382.2	351.3
Max. bending moment	M_m	(kNm/m)	455.7	455.7	455.7	455.7	455.7	460.1	456.5

Note: All methods in columns (4) to (8) are generalized and extended (GE)

5 VALIDATION OF THE METHOD

A comprehensive set of results has been calculated for comparisons in order to validate the performance of the proposed method. Four cases are presented. In the first case, a cantilever reinforced concrete retaining structure of a certain width, embedded in homogeneous cohesionless ground of certain properties at a certain soil-wall friction, was analyzed, where the height of the retaining structure and surcharge loading had been altered. The remaining three cases concerned a cantilever embedded retaining structure of certain height, where analyses were performed for different combinations of normalized c^* and p^*. The variation of (h/d), M^*_m and T^*_m with K is given in the form of diagrams.

5.1 CASE 1

A cantilever embedded reinforced concrete retaining structure (1.0 m in width) for the protection of a construction pit in homogeneous cohesionless ground was considered. The following ground properties were considered: $\varphi = 49.5°$, $c = 0$, $\delta = 20$ kN/m³, and friction between soil and wall $\delta = \varphi$. Three examples were analyzed:

(a) $h = 10.0$m, $p = 0$,
(b) $h = 10.5$m, $p = 10$ kPa
(c) $h = 11.0$m, $p = 20$ kPa.

The results of analyses are presented in Table 2.

The results of analyses for example (a) show, that in ideal homogeneous cohesionless ground the classical analytical methods (UK simplified, UK full and USA) give similar results. They differ from the solutions of more recent methods (King, Day, FE and Proposal) in required embedment depths and maximum internal shear forces. The differences in embedment depths are up to 61%, for maximum internal shear forces up to 206%, and for bending moments up to 1.6% with regard to the smallest values.

In examples (b) and (c) the weight of the ground at the toe of excavation was substituted with the pertinent surcharge loading (soil without shear strength). The differences with the smallest values for embedment depths are up to 76% in example (b) and grow up to 90% in example (c), for maximum internal shear forces up to 219% and 243%, and for bending moments up to 1.5% and 1%. In these cases King's and Day's method exhibit unacceptable solutions, because the required embedment depth is smaller than that of a ground with very high pressure resistance at the dredge level. For such

cases, the results of analyses obtained by the two newer methods are comparable with the results obtained using classical methods. It can be concluded from the above examples, that all the presented methods give practically the same values of bending moments. This is due to the fact that bending moments depend mostly on wall height.

When the surcharge loading in the excavation pit at the dredge line level is considered, only the results of the proposed method are comparable with the results of FEM elasto-plastic analyses.

5.2 CASE 2

The limit states of a rigid cantilever reinforced concrete retaining structure embedded in homogeneous cohesionless ground were considered. The numerical analyses were done for ground with friction angles from $\varphi = 10°$ to $\varphi = 50°$ in steps of 2.5°, cohesion $c = 0$, and without surcharge loading. The analyses were performed for all considered methods. In all analyses the rigid retaining structure of total height $h + d = 10.0$ m, friction between soil and wall $\delta = \varphi$, dilatation angle $\psi = \varphi/2$, and unit weight $\gamma = 20$ kN/m³ were considered. Fig. 9 shows the distribution of horizontal soil pressures acting on the retaining structure in homogeneous ground for $\varphi = 20$, 35 and 50°. The solution according to FEM is presented in the same way as the results published by Day (1999). The excavation depths for each individual method are presented in the same diagram.

It can be concluded from the net pressure distributions in Fig. 9, that the pressure distribution given by the proposed method agrees very well with the calculated net pressure points using FEM (Day 1999). Fig. 10a presents the variation of the required normalized values of embedment depth d^* ($d^* = d/h$), maximum bending moments M^*_m, and maximum shear forces T^*_m with parameter K.

It is evident from Fig. 10a that the results of the proposed method are in agreement with the results of FE analyses and the solutions of Day (1999). The latest solutions show larger deviations at higher values of K ratios, which do not appear in practice. However, these deviations arise in further analyses for layered ground and when surcharge loading is presented.
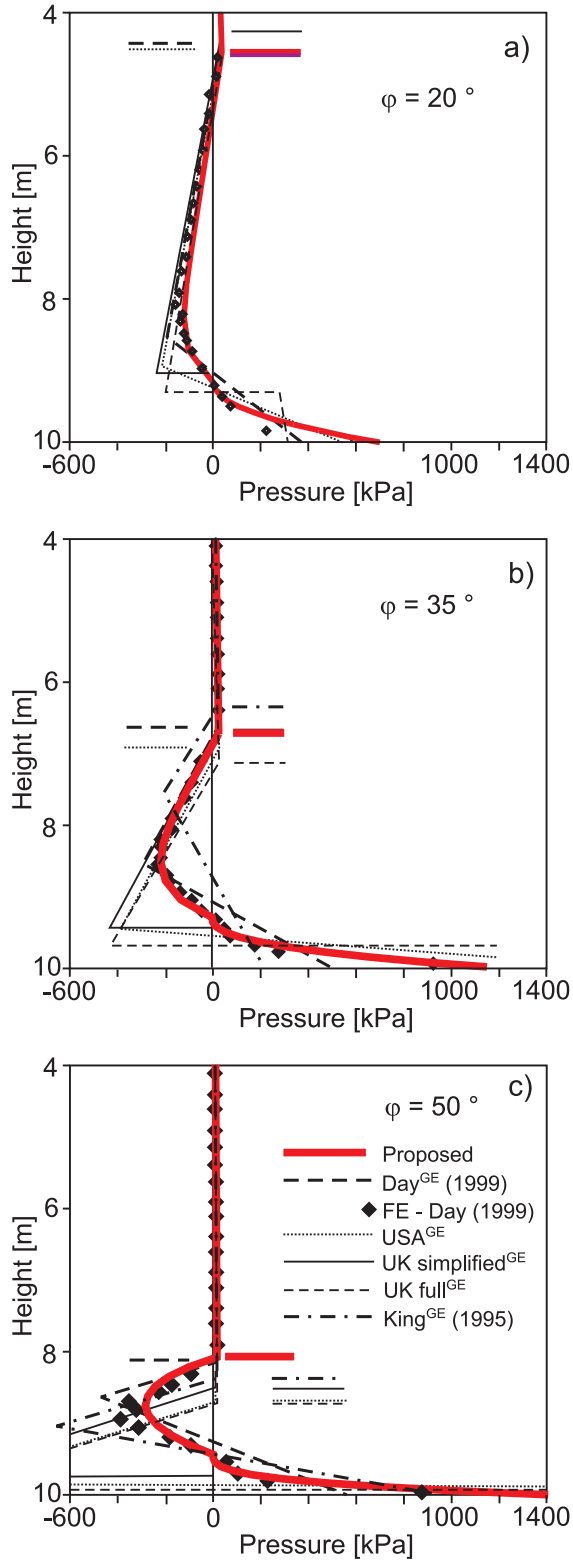
Figure 9. Net Pressure Distribution:
(a) $\varphi = 20°$
(b) $\varphi = 35°$
(c) $\varphi = 50°$

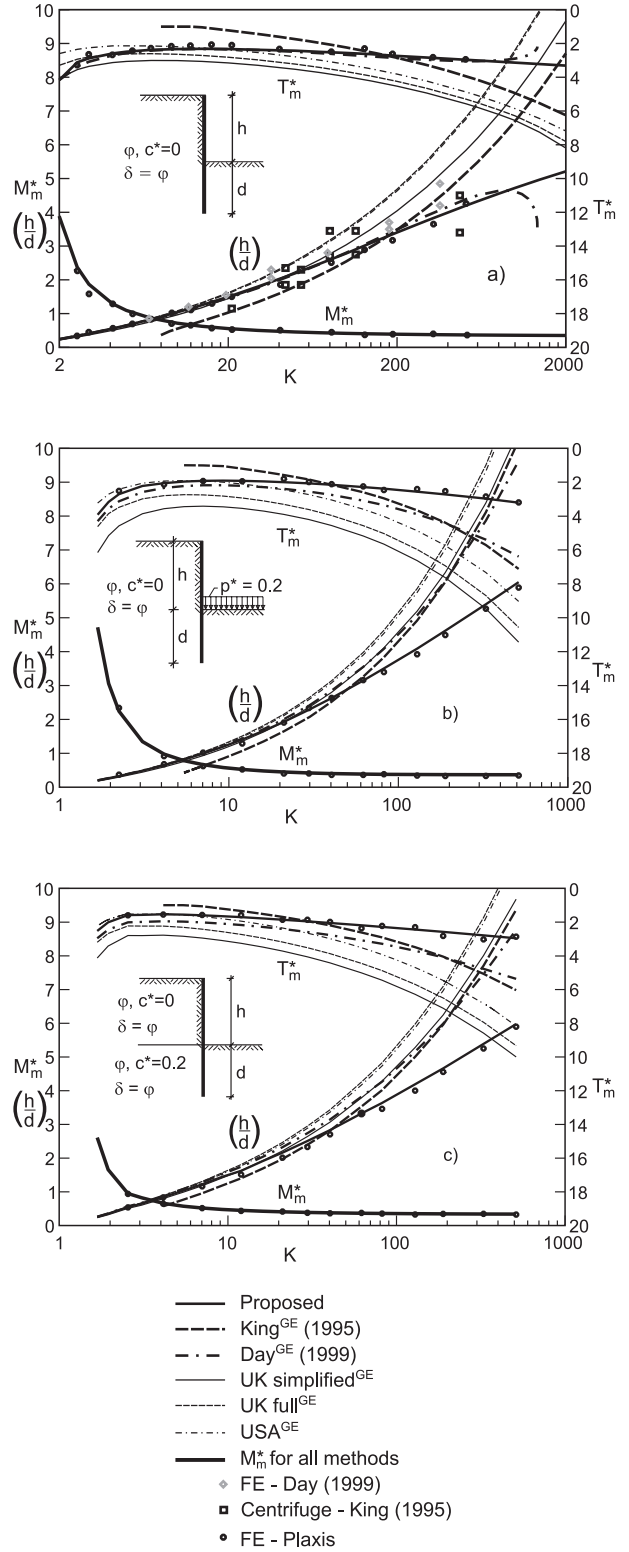**Figure 10**. Variation of (h/d), M^*_m and T^*_m with K for:
a) $c^* = q^* = p^* = 0$
b) $c^* = q^* = 0$ and $p^* = 0.2$
c) $p^* = q^* = 0$ and $c^* = 0.2$

It is evident from Fig. 10a that the results of the proposed method are in agreement with the results of FE analyses and the solutions of Day (1999). The latest solutions show larger deviations at higher values of *K* ratios, which do not appear in practice. However, these deviations arise in further analyses for layered ground and when surcharge loading is presented.

5.3 CASE 3

The limit states of the rigid cantilever reinforced concrete retaining structure embedded in homogeneous cohesionless ground were considered again. The influence of surcharge loading in front of the retaining structure at the toe of the construction pit was considered, too. In geotechnical practice such loading represents the influences of soil layers with low pressure resistance, which are located above the foreseen embedment depth of the retaining structure. Fig. 10b presents the variation of the required normalized embedment values of the depth d^* ($d^* = d/h$), maximum bending moments M^*_m, and maximum shear forces T^*_m with parameter *K*. It is evident from Fig. 10b that only the results of the proposed method agree with the numerical results of FEM analyses.

5.4 CASE 4

The limit states of the rigid cantilever retaining structure in homogeneous ground were considered further, where soils under the dredge level have a part of the cohesion shear strength of the upper layer, $c^* = 0.2$. Fig. 10c presents the variation of the required embedment depth normalized values d^* ($d^* = d/h$), maximum bending moments M^*_m, and maximum shear forces T^*_m with parameter *K*. It is again evident from Fig. 10c that only the results of the proposed method agree with the numerical results of FE analyses.

6 CONCLUSIONS

The results of analyses show that, due to the interaction between rigid cantilever retaining structures and the ground, the entire passive resistance is not actually mobilized, as is considered in classical methods for retaining structure analyses (UK simplified, UK full and USA).

The greatest differences are exhibited for structures embedded in soils with high shear strength when higher friction between the structure and the ground is consid-

ered. Furthermore, the largest differences are obtained in the region of the wall's fictitious rotation point at embedment depth, and at the toe of the embedded retaining structure.

This paper presents the equations of the existing methods in generalized form, which enables analyses of retaining structures considering layered ground and surcharge loading.

Based on the performed analyses it can be established that the results of the proposed method agree very well with the results of finite element elastoplastic analysis and with the results of centrifuge tests. All the existing methods for cantilever pile wall analysis, as well as the proposed one, give nearly the same values for maximum bending moments. Furthermore, only the proposed method yields a reliable embedment depth and maximum internal shear force and does not underestimate embedment depths and overestimate internal shear forces, as do the existing methods.

The special benefit of this method is due to the realistic values for internal shear forces, which are, as a rule, strongly overestimated in the remaining methods. This benefit leads to a more economical design of pile walls, since larger pile spacing is possible. Consequently, the total bearing capacity of the reinforced concrete section can be exploited and a comparable safety of ground bearing capacity and strength of structure sections can be reached.

In practice, almost all retaining structures are erected in layered ground; the existing methods only give exact solutions for retaining structures in cohesionless ground. Therefore, this proposed method is more convenient and more applicable in the analysis and design of cantilever structures in geotechnical practice.

APPENDIX I.

REFERENCES

Bica, A. V. D., and Clayton, C. I. R. (1989). Limit equilibrium design methods for free embedded cantilever walls in granular materials. *Proc. Instn Civ. Engrs* Part 1, 879-989.

Bica, A. V. D. and Clayton, C. I. R. (1993). The preliminary design of free embedded cantilever walls in granular soil. *Retaining structures*, C. R. I. Clayton, ed., Thomas Telford, London, England, 731-740.

Bowles, J. E. (1988). *Foundation analysis and design*, 4th Ed., McGraw-Hill Book Co., New York, N.Y., 613-618.

Day, R. A. (1999). Net pressure analysis of cantilever sheet pile walls. *Geotechnique*, London, England, 49(2), 231-245.

Fang, Y. S., Chen, T. J., and Wu, B. F. (1994). Passive earth pressures with various wall movements. *J. Geotech. Engng Div.*, ASCE, 120(8), 1307-1323.

Kérisel, J., and Absi, E. (1990). *Tables for the calculation of passive pressure, active pressure and bearing capacity of foundations*. Gauthier-Villard, Paris, France.

King, G. J. W. (1995). Analysis of cantilever sheet-pile walls in cohesionless soil. *J. Geotech. Engng Div.*, ASCE, 121(9), 629-635.

Lyndon, A., and Pearson, R. A. (1985). Pressure distribution on a rigid retaining wall in cohesionless material. *Proc., Int. Symp. on Application of Centrifuge Modeling to Geotech. Design*, W. H. Craig, ed., A. A. Balkema, Rotterdam, The Netherlands, 271-280.

Padfield, C. J., and Mair, R. J. (1984). Design of retaining walls embedded in stiff clays. *CIRIA Report 104*, London, Constr. Industry Res. and Information Assoc. (CIRIA), London, England.

PLAXIS user's manual, version 7 (1998). R. B. J. Brinkgreve, and P. A. Vermeer, eds., A. A. Balkema, Rotterdam, The Netherlands

Rowe, P. W. (1951). Cantilever sheet piling in cohesionless soil. *Engrg.*, London, England , (Sept.), 316-319.

APPENDIX II.

NOTATION

The following symbols are used in this paper:

a = distance of the resulting force of active pressures from the dredge line (see Figs. 2 and 3);

a^* = normalized quantity defined as ratio a/h;

c^* = normalized quantity defined as ratio $2c/(\gamma h)$;

C_1, C_2 = integration constants (see Eq. 16);

d = total embedment depth (see Figs. 2 and 3);

d_1, d_2 = partial embedment depths (see Figs. 2 and 3);

d^*, d_1^*, d_2^* = normalized quantity defined as ratios d/h, d_1/h and d_2/h;

E = resulting force of active pressures above dredge line (see Figs. 2 and 3);

E^* = normalized quantity defined as ratio $2E/(\gamma h^2 K_{ay})$;

E_{50}^{ref} = secant stiffness in standard drained triaxial test at the reference pressure;

E_{oed}^{ref} = tangent stiffness for primary oedometer loading at the reference pressure;

E_{ur}^{ref} = unloading / reloading stiffness in Hardening-Soil model (considered $E_{ur}^{ref} = 3 E_{50}^{ref}$);

h = height of the retaining structure (see Figs. 2 and 3);

h_c = critical (allowable) excavation depth;

K = ratio between K_{py} and K_{ay};

K_{pc}, K_{ac} = coefficient of passive and active earth pressure for influence of cohesion;

K_{py}, K_{ay} = coefficients of passive and active earth pressure for influence of soil weight;

K_{pq} = coefficient of passive earth pressure for influence of surcharge;

m = parameter in elasto-plastic Hardening-Soil model (it is the input parameter in the relationship for stress dependent stiffness according to a power law) and parameter that defines family of exponential functions in proposed method;

n = parameter that defines family of exponential functions in proposed method;

M_m = maximum value of bending moment;

M_m^* = normalized value of maximum bending moment;

p_0 = pressure on the pile wall at the dredge line (see Figs. 2 and 3);

p_0^* = normalized quantity defined as ratio $2p_0/(\gamma h K_{ay})$;

p_b = net pressure at the toe of the pile wall (see Figs. 2 and 3);

p_b^* = normalized quantity defined as ratio $2p_b/(\gamma h K_{ay})$;

p^{ref} = reference pressure in elasto-plastic Hardening-Soil model;

R_f = parameter in elasto-plastic Hardening-Soil model that defines failure ratio q_f/q_a (ultimate deviatoric stress / asymptotic value of the shear strength), is derived from the Mohr-Coulomb failure criterion;

R^*_1 = normalized resulted horizontal force in region of depth d_1;

R^*_2 = normalized resulted horizontal force in region of depth d_2;

$M^{*0}_{R^*_1}$ = normalized resulted moment of activated resistances in region of depth d_1;

q^* = normalized quantity defined as ratio $2q/(\gamma h)$;

T_m = maximum value of shear force;

T^*_m = normalized value of maximum shear force;

t = thickness of the retaining structure;

t^* = normalized quantity defined as ratio t/h;

u = horizontal displacement;

u^* = normalized horizontal displacement;

u^*_0 = normalized horizontal displacement at the top of the retaining structure;

x^*_m = distance of the point where maximum bending moment acts measured from the bottom of excavation;

z = independent variable that denotes depth;

$z^*_{R^*_2}$ = distance of the resulted horizontal force;

γ = unit weight of the soil;

γ^* = ratio between average unit weight of the backfill ground above dredge line and the unit weight of the ground under dredge line;

δ = friction angle at the soil-structure interface;

ε = experimentally determined parameter that defines depth at which activated contact stresses in front of and behind embedded pile are balanced wall (see Fig. 3);

v_{ur} = Poisson's ratio for unloading-reloading in Hardening-Soil model (considered $v_{ur} = 0.2$);

φ = angle of internal friction of the soil; and

ψ = angle of dilatation of the soil.